ELSEVIER

Surface Science 490 (2001) 315–326

SURFACE SCIENCE

www.elsevier.com/locate/susc

Formation of Mo and MoS_x nanoparticles on Au(1 1 1) from $Mo(CO)_6$ and S_2 precursors: electronic and chemical properties

José A. Rodriguez *, Joseph Dvorak, Tomas Jirsak, Jan Hrbek *

Department of Chemistry, Brookhaven National Laboratory, Bldg. 555, P.O. Box 5000, Upton, NY 11973-5000, USA

Received 9 March 2001; accepted for publication 8 June 2001

Abstract

$Mo(CO)_6$ can be useful as a precursor for the preparation of Mo and MoS_x nanoparticles on a Au(1 1 1) substrate. On this surface the carbonyl adsorbs intact at 100 K and desorbs at temperatures lower than 300 K. Under these conditions, the dissociation of the $Mo(CO)_6$ molecule is negligible and a desorption channel clearly dominates. An efficient dissociation channel was found after dosing $Mo(CO)_6$ at high temperatures (>400 K). The decomposition of $Mo(CO)_6$ yields the small coverages of pure Mo that are necessary for the formation of Mo nanoclusters on the Au(1 1 1) substrate. At large coverages of Mo (>0.15 ML), the dissociation of $Mo(CO)_6$ produces also C and O adatoms. Mo nanoclusters bonded to Au(1 1 1) exhibit a surprising low reactivity towards CO. Mo/Au(1 1 1) surfaces with Mo coverages below 0.1 ML adsorb the CO molecule weakly (desorption temperature < 400 K) and do not induce C–O bond cleavage. These systems, however, are able to induce the dissociation of thiophene at temperatures below 300 K and react with sulfur probably to form MoS_x nanoparticles. The formed MoS_x species are more reactive towards thiophene than extended MoS_2(0 0 0 2) surfaces, MoS_x films or MoS_x/Al_2O_3 catalysts. This could be a consequence of special adsorption sites and/or distinctive electronic properties that favor bonding interactions with sulfur-containing molecules. © 2001 Elsevier Science B.V. All rights reserved.

Keywords: Carbon monoxide; Gold; Molybdenum; Sulphides; Sulphur; Surface chemical reaction; Synchrotron radiation photoelectron spectroscopy

1. Introduction

MoS_2 is the most widely used metal sulfide catalyst in the chemical and petroleum refining industries [1,2]. Among other reactions, molybdenum sulfide is able to catalyze the synthesis of alcohols from CO [3], the isomerization and hydrogenation of olefins [4], and the hydrotreatment of oil-derived feedstocks (hydrodesulfurization (HDS), hydrodenitrogenation and hydrodeoxygenation processes) [5]. By far the most important application of MoS_2 catalysts involves HDS processes, where sulfur-containing molecules are removed from petroleum by reaction with hydrogen to form H_2S and hydrocarbons [5–8]. Sulfur-containing compounds are present as impurities in all crude oils [2]. These impurities have a very negative impact on the

* Corresponding authors. Tel.: +1-631-3442246; fax: +1-631-3445815.

E-mail address: rodrigez@bnl.gov (J.A. Rodriguez).

0039-6028/01/$ - see front matter © 2001 Elsevier Science B.V. All rights reserved.
PII: S0039-6028(01)01347-4

processing of oil-derived chemical feedstocks (poisoning of hydrocarbon reforming catalyst [9] and equipment corrosion [2]) and degrade the quality of the air by forming sulfur oxides (SO_x) during the burning of fuels [10]. New environmental regulations emphasize the importance of more efficient technologies for removing the sulfur from the oil [11]. This fact has motivated a strong interest in enhancing the HDS catalytic activity of molybdenum sulfide by preparing novel structures or spacial arrays of this material [5–7,12].

In the emerging field of nanotechnology a goal is to make nanostructures with interesting functional properties. In principle, the chemical properties of a material can change when the "length scale" varies from a bulk sample to nanoparticles. Clusters of molybdenum sulfide can expose adsorption sites or exhibit electronic states that are not seen on surfaces of bulk MoS_2 [13]. Recently, the preparation of MoS_2 nanoclusters on a Au(1 1 1) substrate has been reported [12]. The MoS_2 nanoclusters were prepared by evaporation of Mo in an atmosphere of H_2S. The nanoclusters were lying flat on the elbows of the Au herringbone structure exhibiting a triangular shape with a side length of ~30 Å [12]. The basal (0 0 0 1) plane of the MoS_2 particles was oriented parallel to the Au(1 1 1) substrate.

The clean Au(1 1 1) surface exhibits a long range $22 \times \sqrt{3}$ reconstruction with atoms in the top layer contracted laterally relative to the bulk [14–16]. Adatoms alternate in registry with the subsurface layer creating parallel lines of misfit dislocations with a periodicity of 6.3 nm. To relieve the stress isotropically a superstructure is formed with stress domains alternating by ±120° in a zigzag pattern usually referred to as a herringbone structure [14–16]. This herringbone structure can be used as a template for adsorption and directed growth of metal nanoclusters [17]. Experiments of scanning tunneling microscopy (STM) show that vapor deposition of Ni, Fe, Co, Mo and Pd on Au(1 1 1) leads to formation of nanoclusters or small islands of the admetal on the "elbows" of the herringbone structure [12,18–21]. Since gold is a chemically inert element [22,23], a gold template can be ideal for growing and probing the chemical reactivity of metal, oxide and sulfide nanoparticles [17]. We have started a research program using metal carbonyls as precursors in the synthesis of nanoparticles on well-defined templates. Recently, $Mn_2(CO)_{10}$ was used as a precursor for synthesizing MnO nanoparticles on a Pt(1 1 1) substrate [24].

In this work, we show that $Mo(CO)_6$ and S_2 are useful as precursors for the preparation of Mo and MoS_x aggregates on Au(1 1 1). Synchrotron based photoemission is used to study the chemistry of $Mo(CO)_6$ on Au(1 1 1), and examine the electronic properties of Mo and MoS_x on the gold substrate. The chemical properties of Mo and MoS_x aggregates are probed by CO and thiophene (a typical test molecule in HDS studies [5,13,25,26]) chemisorption.

2. Experimental methods

The experiments described in Section 3 were performed in an ultra-high vacuum (UHV) chamber that is part of the U7A beam line of the National Synchrotron Light Source (NSLS) at Brookhaven National Laboratory (BNL). This UHV chamber is equipped with a hemispherical electron-energy analyzer with multichannel detection, optics for low-energy electron diffraction (LEED), and a quadrupole mass spectrometer. All the reported Mo 3d, C 1s, Au 4f and S 2p photoemission spectra were collected at a photon energy of 370 eV. A photon energy of 625 eV was used to collect O 1s spectra. The binding energy scale in the photoemission data was calibrated by measuring the position of the Fermi edge.

The Au(111) crystal was mounted on a manipulator capable of resistive heating to 1200 K and cooling to 80 K. The sample was a disk (~10 mm in diameter and 2 mm in thickness) held tightly by a Ta wire imbedded in a groove machined around the crystal edge. This Ta wire was spot-welded to two Ta rods directly attached to the manipulator. The temperature was measured by a type C thermocouple placed into the groove at the edge of the crystal. A similar sample set-up has been used in previous studies [22]. The Au(1 1 1) surface was cleaned of S, C, O, or Mo by Ne^+ sputtering at 700 K, followed by annealing at higher temperatures

(~1000 K) to obtain the distinctive LEED pattern of the reconstructed Au(1 1 1)-22 × $\sqrt{3}$ surface [12,14].

$Mo(CO)_6$ (K&K Laboratories, >99% purity) was placed in an independently pumped glass test tube [27]. Dosing of $Mo(CO)_6$ was performed through a glass capillary array doser facing the Au(1 1 1) crystal at a distance of ~2 mm [27]. The coverages of Mo on the gold substrate were estimated using the relative intensity of the Mo 3d and Au 4f core levels together with changes in the line shape of the valence region [28]. Due to the depth sensitivity of the photoelectrons, the estimated Mo coverages could represent lower limits to the exact values if the metal adlayer forms three-dimensional structures. Clean Au(1 1 1) and Mo nanoparticles supported on this substrate were exposed to S_2 at 300 K. S_2 gas was generated in situ by decomposing silver sulfide in a solid-state electrochemical cell, Pt/Ag/AgI/Ag_2S/Pt [29,30]. The interaction of sulfur with Mo/Au(1 1 1) led to formation of MoS_x. Thiophene (Aldrich, >99% purity) was dosed to Au(1 1 1), Mo/Au(1 1 1) and MoS_x/Au(1 1 1) surfaces at 100 K from the background by backfilling the UHV chamber.

3. Results

3.1. Chemistry of $Mo(CO)_6$ on Au(1 1 1)

Fig. 1 shows Mo 3d and C 1s spectra acquired after adsorbing a large coverage of $Mo(CO)_6$, 5 L (langmuir) exposure, on Au(1 1 1) at 100 K. The features for the Au 5d band in the valence region (not shown) essentially disappeared upon adsorption of this multilayer of molybdenum carbonyl. Heating from 100 to 200 K produced minor changes in the photoemission spectra. On the other hand, upon heating to room temperature, there was a very large reduction in the Mo 3d and C 1s signals probably due to desorption of $Mo(CO)_6$ [27]. By 300 K, ~0.02 ML of molybdenum were left on the Au(1 1 1) surface and a weak trace of a CO signal was seen in the C 1s spectrum. Final heating to 600 K removed all the C 1s signal leaving ~0.02 ML of Mo on the gold substrate.

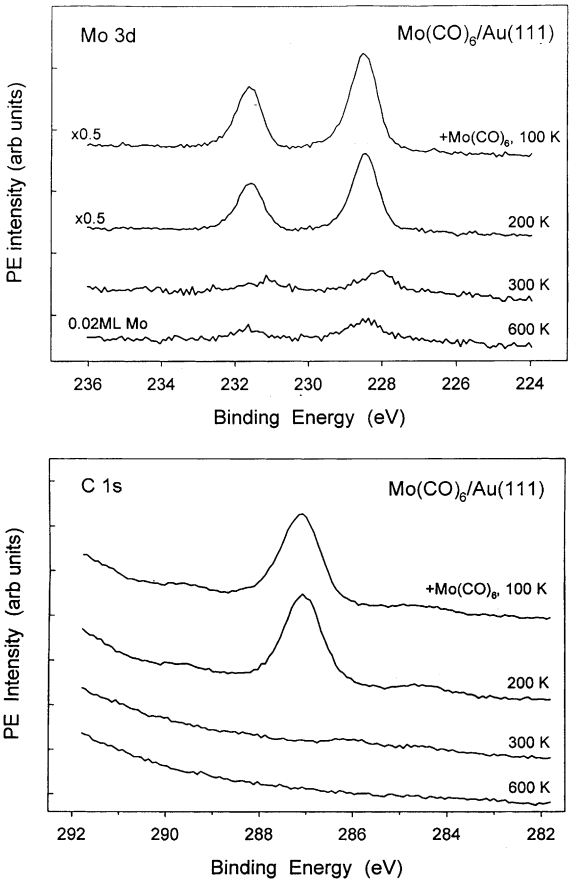

Fig. 1. Mo 3d (top) and C 1s (bottom) photoemission spectra acquired after adsorbing a multilayer of $Mo(CO)_6$ at 100 K on Au(1 1 1), with subsequent heating to 200, 300 and 600 K.

These results indicate that $Mo(CO)_6$ has a very low reactivity on Au(1 1 1) at low temperatures. However, the decomposition of $Mo(CO)_6$ following the procedure shown in Fig. 1 is able to produce a small coverage of molybdenum, and under these conditions the Mo atoms should be forming nanoparticles or very small islands on the "elbows" of the gold herringbone structure as shown by STM experiments [12,18]. In general, vapor deposition of small amounts of Ni, Fe, Co, Mo and Pd on Au(1 1 1) leads to formation of nanoclusters on the "elbows" of the herringbone structure [12,18–21].

A more efficient route for the dissociation of $Mo(CO)_6$ was observed after dosing the metal carbonyl to the Au substrate at a temperature of

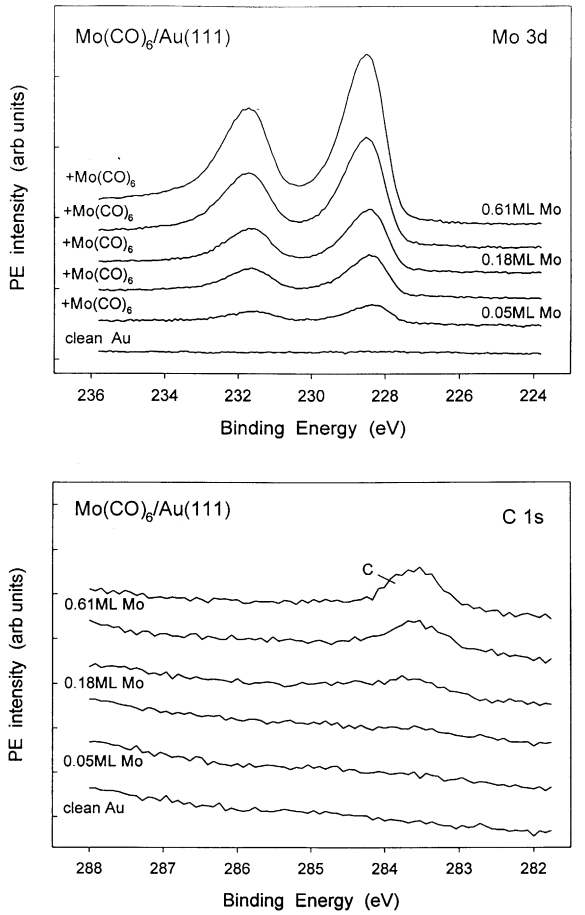

Fig. 2. Mo 3d (top) and C 1s (bottom) photoemission spectra acquired after sucessive doses of $Mo(CO)_6$ to Au(1 1 1) at 500 K. Upon each $Mo(CO)_6$ dose, the sample was heated to 600 K.

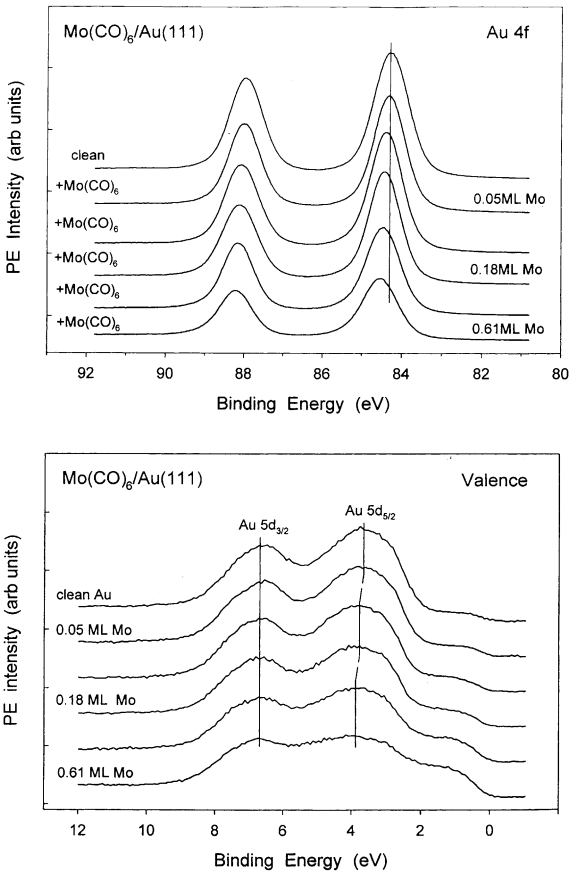

Fig. 3. Au 4f (top) and valence (bottom) photoemission spectra acquired after sucessive doses of $Mo(CO)_6$ to Au(1 1 1) at 500 K. Upon each $Mo(CO)_6$ dose, the sample was heated to 600 K.

500 K. Figs. 2 and 3 show typical photoemission results for this type of experiment. After each dose (10 L) of $Mo(CO)_6$ at 500 K, the sample was briefly annealed to 600 K. The first two doses of $Mo(CO)_6$ in Fig. 2 produced pure Mo/Au(1 1 1) systems that were free of carbon or oxygen as shown by photoemission. (The C 1s and O 1s spectra were collected using photon energies, 370 and 625 eV, for which our instrument can detect C and O coverages in the range of 0.01–0.05 ML without problem [26]). At Mo coverages below 0.1 ML, one can expect nucleation of Mo nanoparticles on the Au(1 1 1) substrate [12,18]. These systems exhibited Mo $3d_{5/2}$ binding energies that were 0.2–0.3 eV higher than those measured in our instrument for bulk molybdenum (228.0 eV [26]). It appears that these Mo structures are not able to dissociate CO like the metal atoms in extended Mo surfaces [23,31]. In Fig. 2, as the coverage of Mo on the gold substrate increases ($\theta_{Mo} > 0.15$ ML), the metal adlayer becomes reactive and there is cracking of CO groups on the surface leaving C and O adatoms. We found that multilayers of molybdenum can be deposited on Au(1 1 1) by decomposition of $Mo(CO)_6$ at 500 K, but this thick metal overlayers contained also atomic C and O impurities.

Fig. 3 displays Au 4f and valence spectra acquired in the same set of experiments that produced the photoemission data in Fig. 2. As Mo is deposited on Au(1 1 1), there is a monotonic

decrease in the intensity of the Au 4f peaks and a shift towards higher binding energy. For a system with 0.61 ML of Mo, the Au 4f features are shifted ~+0.3 eV with respect to the corresponding features of Au(1 1 1). A similar binding energy shift has been observed after depositing Au atoms on a Mo(1 1 0) surface [28]. It probably reflects a Au(5d) → Au(6s, 6p) charge redistribution induced by bimetallic bonding [28]. Previous studies indicate that the photoemission cross-section for the Au 5d band is much larger than that for the Mo 4d band [28]. The 4d band of Mo surfaces extends from 5 to 0 eV with a maximum near 1.5 eV [28]. In the case of clean Au(1 1 1), the emission of electrons between 0 and 2 eV is weak, and the 5d band is located from 2 to 8 eV with two well-defined components ($5d_{3/2}$ and $5d_{5/2}$). In the bottom panel of Fig. 3, the deposition of Mo leads to an increase in the signal between 0 and 2 eV. The position of the Au $5d_{3/2}$ features is almost not affected while there is an increase in the binding energy of the Au $5d_{5/2}$ features. The same trend was found when Au atoms were adsorbed on Mo(1 1 0) [28], and suggests that the formation of Mo–Au bonds is accompanied by a redistribution of electrons around the metal centers.

3.2. Adsorption of CO and thiophene on Mo/Au(1 1 1)

The adsorption of CO (99.99% purity) and thiophene (C_4H_4S, >99% purity) was studied on Mo/Au(1 1 1) surfaces with a molybdenum coverage of ~0.05 ML ($Mo_{0.05}$/Au(1 1 1) in our notation), systems in which Mo nanoparticles should be located on the "elbows" of the gold herringbone structure [12]. We found that these $Mo_{0.05}$/Au(1 1 1) surface were unable to adsorb CO at 300 K after a 100 L dose. In this respect, the bimetallic systems behaves as pure gold [22,23]. Adsorption of CO was observed at 100 K upon a 20 L dose, but the molecule desorbed intact without decomposition upon heating to 300 K. A larger chemical reactivity was observed towards thiophene. Fig. 4 shows S 2p and Mo 3d spectra acquired after adsorbing thiophene on a $Mo_{0.05}$/Au(1 1 1) surface. Upon adsorption of thiophene at 100 K, one sees a well-defined doublet between 166 and 164 eV in

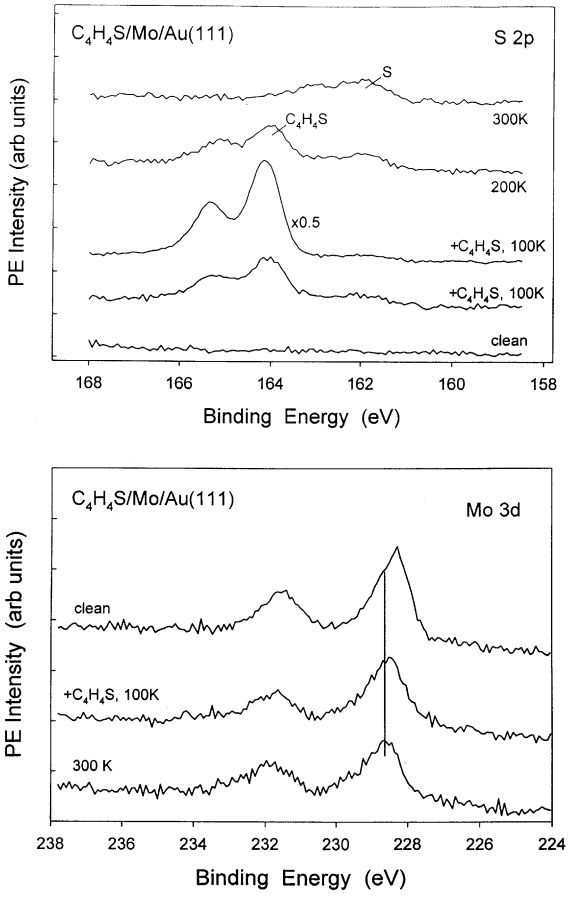

Fig. 4. S 2p (top) and Mo 3d (bottom) photoemission spectra acquired after adsorbing thiophene on a Mo/Au(1 1 1) surface with ~0.05 ML of molybdenum. Thiophene was dosed at 100 K with subsequent heating to 200 and 300 K.

the S 2p region. In addition, weak features are detected around 162 eV, which indicate the dissociation of some C_4H_4S molecules [26]. Heating from 100 to 200 K leads to desorption of physisorbed thiophene [26] and the features for atomic S gain intensity. By 300 K, all the molecular thiophene has disappeared from the surface leaving behind a clear signal for atomic S. The binding energy position of these features is much higher than that seen for S atoms on Au(1 1 1), see below. At the same time, the interaction with thiophene shifts the Mo 3d peaks of the $Mo_{0.05}$/Au(1 1 1) surface towards higher binding energy. Both of these results indicate that thiophene decomposed

on the supported Mo nanoparticles. The products of this decomposition are S and C_xH_y fragments according to photoemission. The reactivity of pure Au(1 1 1) towards thiophene is negligible with the molecule desorbing below room temperature upon adsorption at 100 K [32]. On the other hand, Mo(1 1 0) and Mo(1 0 0) dissociate C_4H_4S at temperatures well below 200 K [26,33].

3.3. Interaction of sulfur with Mo/Au(1 1 1) and formation of MoS_x

Before examining the interaction of sulfur with $Mo_{0.05}$/Au(1 1 1) surfaces, we will focus briefly our attention on the behaviour of the sulfur/Au(1 1 1) system. At the bottom of Fig. 5 is shown a S 2p spectrum taken after saturating a Au(1 1 1) surface with sulfur at 300 K. This complex spectrum contain contribution from at least three species [30,32]. The features near 161 eV correspond to S atoms probably bonded to hollow sites of the gold surface [32]. The strong features from 165 to 163 eV are characteristic of sulfur aggregates (S_n) [30,34]. Heating to 400 K induces desorption of a substantial amount of sulfur as S_2 [32]. By 500 K, only atomic sulfur is bonded to gold and a well-defined doublet is seen between 163 and 161 eV [30,32]. Further heating leads to a monotonic decrease in the S 2p signal and at temperatures above 800 K, the coverage of sulfur on the Au(1 1 1) surface is negligible.

Figs. 6 and 7 display photoemission results for the adsorption of sulfur on a $Mo_{0.05}$/Au(1 1 1) system. The S 2p spectrum at 300 K (Fig. 6) exhibits features that are similar to those found for sulfur/Au(1 1 1) in Fig. 5, with the exception of a stronger intensity in the region around 162.5 eV.

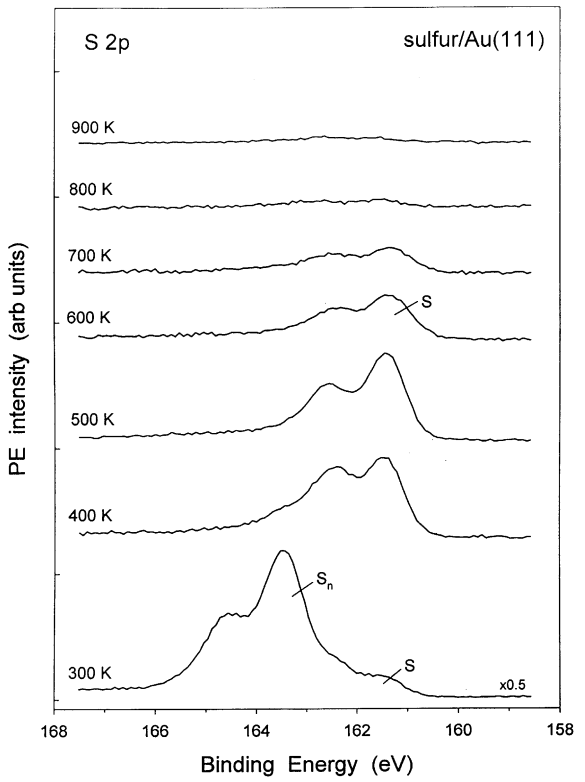

Fig. 5. S 2p photoemission spectra for the adsorption of sulfur on Au(1 1 1).

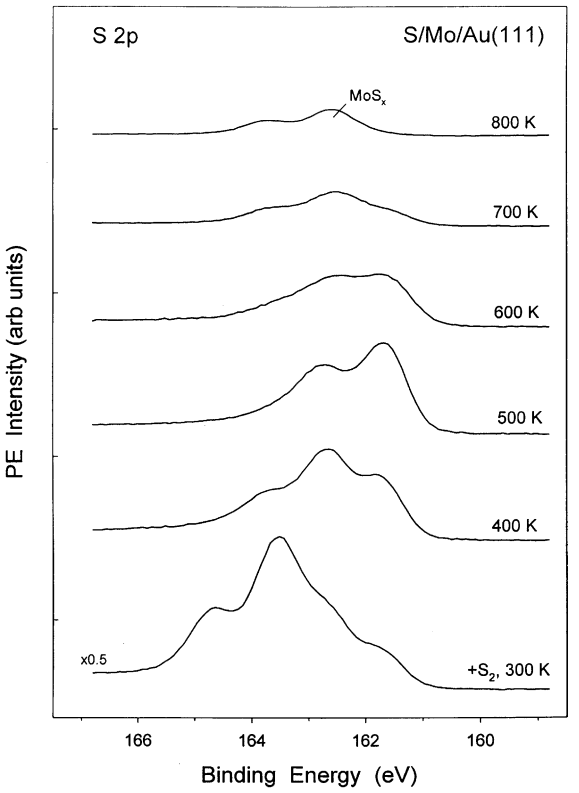

Fig. 6. S 2p photoemission spectra for the adsorption of sulfur on a $Mo_{0.05}$/Au(1 1 1) surface. Sulfur was dosed at 300 K and the sample was then annealed to the indicated temperatures.

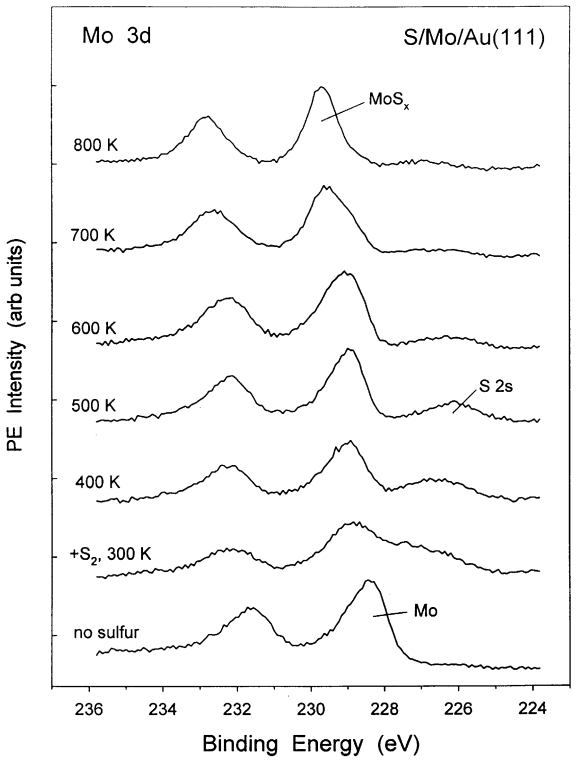

Fig. 7. Mo 3d photoemission spectra for the adsorption of sulfur on $Mo_{0.05}$/Au(1 1 1) surface. Sulfur was dosed at 300 K and the sample was then annealed to the indicated temperatures.

This new signal is probably due to S atoms bonded to the Mo nanoparticles [35,36]. Heating from 300 to 400 K induces desorption of S_2 and produces a drastic change in the line shape of the S 2p spectrum. At this point, the surface contains only S atoms bonded to Au or Mo (i.e. no S_n aggregates). Additional heating leads to desorption of the sulfur that is bonded to gold and, by 800 K, the S 2p region shows a well-defined doublet that is not seen for pure sulfur/Au(1 1 1) in Fig. 5. This doublet is close to the binding-energy positions found for S stoms in MoS_x films [35,36].

The Mo 3d data in Fig. 7 confirm that MoS_x is formed upon heating the S/Mo/Au(1 1 1) surface to elevated temperatures. Initially, the deposition of sulfur at 300 K induces an attenuation of the Mo 3d signal and extra features appear near 226 eV due to the S 2s core level. After heating to 400 K, part of the sulfur has desorbed (see Fig. 6) and the Mo 3d features are clearly shifted by $\sim$+0.7 eV with respect to those of the $Mo_{0.05}$/Au(1 1 1) surface. This binding energy shift is smaller than that expected for the formation of MoS_x ($\sim$1.2–1.4 eV [35–37]), and could come from the chemisorption of S on the Mo nanoparticles. At temperatures above 500 K, there is a broadening of the Mo 3d peaks as a consequence of MoS_x formation. The spectrum taken after heating to 800 K contains mainly one type of molybdenum species, with peak position that match well those reported for molybdenum sulfide [37]. We do not have microscopy data for this system, but the overlayer of MoS_x probably consists of nanoparticles located on the "elbows" of the Au herringbone structure [12]. In our studies and in Ref. [12], the final product is MoS_x and the gold substrate is annealed at high temperatures to obtain the most stable configuration of the MoS_x/Au(1 1 1) system.

3.4. Chemistry of thiophene on MoS_x/Au(1 1 1)

In general, we found that MoS_x aggregates deposited on Au(1 1 1) were able to dissociate thiophene upon adsorption at room temperature. No dissociation of C–S bonds was seen when the molecule were adsorbed at 100 K. Figs. 8 and 9 show C 1s and S 2p spectra collected after adsorbing C_4H_4S on the MoS_x/Au(1 1 1) system generated in the experiments of Figs. 6 and 7. Upon adsorption of submonolayer coverages of thiophene at 100 K, there is a single peak in the C 1s region and new features are found in the S 2p spectrum (166–164 eV) due to chemisorbed C_4H_4S. Heating from 100 to 180 K induces minor changes in the C 1s spectrum and extra signal starts to appear near 161 eV in the S 2p region due to atomic S produced by the decomposition of thiophene. This signal increases when the sample temperature is raised to 250 K, but most of the thiophene desorbs into gas phase. After final heating to 350 K, the photoemission data point to the presence of MoS_x, C_xH_y and S on the Au(1 1 1) substrate. The reactivity of pure Au(1 1 1) towards thiophene is negligible [32]. In contrast, Mo/Au(1 1 1) and MoS_x/Au(1 1 1) dissociate C_4H_4S at temperatures well below 300 K.

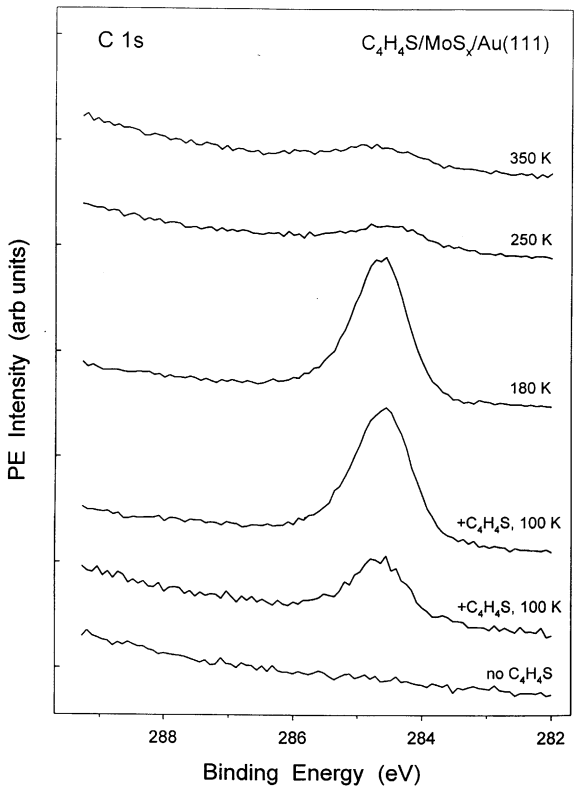

Fig. 8. C 1s photoemission spectra for the adsorption of thiophene on a MoS_x/Au(1 1 1) surface with 0.05 ML of molybdenum. Thiophene was dosed at 100 K with subsequent annealing to 180, 250 and 350 K.

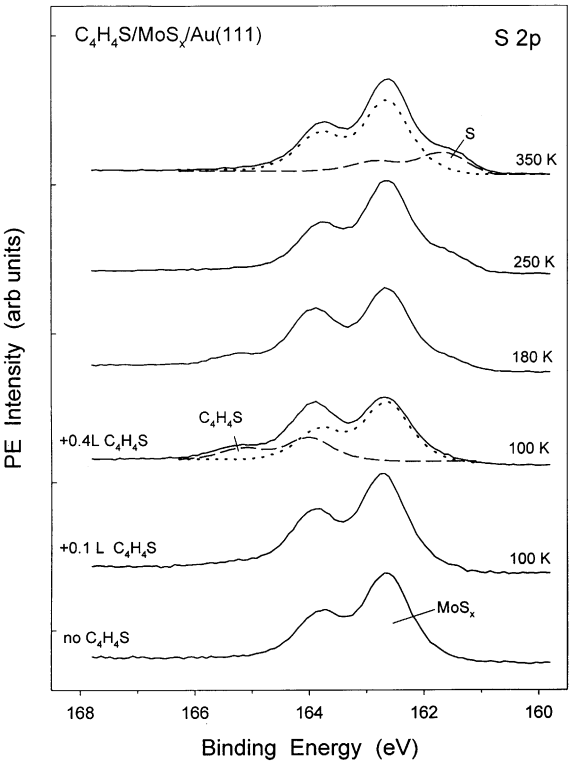

Fig. 9. S 2p photoemission spectra for the adsorption of thiophene on a MoS_x/Au(1 1 1) surface with 0.05 ML of molybdenum. Thiophene was dosed at 100 K with subsequent annealing to 180, 250 and 350 K. The dashed and dotted traces under the third and top spectra show the deconvolution [30,34] of the raw data in two doublets that correspond to C_4H_4S (Fig. 4), MoS_x [35,36], or S adatoms (Figs. 5 and 6).

4. Discussion

Transition metal carbonyls are relevant for a fundamental understanding of substrate–adsorbate systems and for applications in catalysis and thin film technology. The use of metal carbonyls as precursors of heterogeneous catalysts (both mono- and bi-metallic) has been suggested [38] and later explored experimentally [39,40]. This class of compounds has also been used for thin metal film deposition on diverse substrates [41,42]. Several previous studies have examined the interaction of metal carbonyls with metal surfaces: $Ni(CO)_4$ on Pd and Ir [43], $Ni(CO)_4$ on Ni(1 1 1) [44], $Fe(CO)_5$ on Ag(1 1 0) [42] and Ni(1 0 0) [45], $Cr(CO)_6$ on Ni(1 0 0) [45] and Pd(1 0 0) [46], $Mn_2(CO)_{10}$ on Pt(1 1 1) [24], $Ru_3(CO)_{12}$ on Ru(0 0 0 1) [27] and Co(0 0 0 1) [47], $Mo(CO)_6$ on Cu(1 1 1) [48] and Ag(1 1 1) [49], and $W(CO)_6$ on Ni(1 0 0) [50] and W(1 1 0) [51]. The type of chemistry observed varies with the reactivity of the carbonyl compound and metal surface. For example, Ni(1 0 0) is able to decompose $Fe(CO)_5$, $Cr(CO)_6$, $Mo(CO)_6$ and $W(CO)_6$ [45,50]. The initial adsorption of these metal carbonyls is mostly molecular at low temperatures (<200 K), but complete decarbonylation to the naked metal takes place in all cases upon thermal activation [45,50]. A similar trend has been reported for the adsorption of $Ru_3(CO)_{12}$ on Co(0 0 0 1) [47] and $Mo(CO)_6$ on Cu(1 1 1) [48]. Surfaces of early-transition metal like W(1 1 0) are very reactive toward metal carbonyls even at low temperatures [51]. The opposite is seen for $Mo(CO)_6$ on Ag(1 1 1) [49]. On this surface, the

carbonyl adsorbs intact and desorbs at temperatures below 300 K. Our results show a similar behavior for $Mo(CO)_6$ on Au(1 1 1), where the dissociation of the molecule below room temperature is negligible and a desorption channel clearly dominates. The low chemical reactivity of Ag [23,49] and Au [22,23] makes difficult the dissociation of metal carbonyls on surfaces of these metals. For the $Mo(CO)_6$/Au(1 1 1) system, however, we found an efficient dissociation channel at high temperatures (>400 K). This is probably a consequence of a better energy transfer between the surface and carbonyl molecule.

Recently, we have started a research program using metal carbonyls as precursors in the synthesis of nanoparticles on well-defined templates. Since gold is a chemically inert element [22,23], a Au(1 1 1) template can be useful for growing and probing the intrinsic reactivity of metal, oxide, sulfide and carbide nanoparticles [17]. Indeed, vapor deposition of Ni, Fe, Co, Mo and Pd on Au(1 1 1) leads to formation of nanoclusters of the admetals on the "elbows" of the substrate herringbone structure [12,18–21]. Our results show that the decomposition of $Mo(CO)_6$ yields the small coverages of pure Mo necessary for the preparation of metal nanoparticles. It can be expected that this also will be the case when using other metal carbonyls as precursors [17]. Carbonyl compounds naturally provide starting materials for selective metal deposition and nanoparticle growth on surface templates [17,24]. The metal nanoclusters deposited by this approach can undergo additional chemical treatment and be transformed into sulfide, oxide or carbide nanoparticles [17,24]. The photoemission results in Section 3 show that $Mo(CO)_6$ and S_2 are useful as precursors for the preparation of MoS_x aggregates in general. This offers an alternative route to the method employed in Ref. [12], where MoS_2 nanoclusters were prepared on Au(1 1 1) by evaporation of Mo in an atmosphere of H_2S. We also found that MoO_x and MoC_x aggregates can be grown by combining $Mo(CO)_6$ and O_2 or C_2H_2 as precursors.

Mo nanoparticles bonded to Au(1 1 1) exhibit a surprising low reactivity towards CO. Extended surfaces of molybdenum, (1 1 0) and (1 0 0) faces for example, bond CO strongly and dissociate the molecule into C and O atoms [23,31]. In contrast, Mo/Au(1 1 1) surfaces with Mo coverages below 0.1 ML adsorb the CO molecule weakly and do not induce C–O bond cleavage. This could be a consequence of electronic perturbations induced on Mo by bimetallic bonding. The photoemission data in Section 3.1 show core level shifts that suggest a redistribution of electrons around the bonded metals. Among the transition metals, gold has the largest Pauling electronegativity [52]. From this, one could expect a net Mo → Au charge transfer [52–54]. But the charge redistribution around the Mo–Au bonds is more complex than this [28]. In previous studies for bulk alloys, it has been shown that Au can act as a 5d-electron donor and a (6s,6p)-electron acceptor when forming intermetallic compounds [53–56]. Ab initio Hartree–Fock (HF) calculations for small AuMo clusters [28] show inter- and intra-atomic electron transfers: Au(5d) → Mo(4d,5s), Mo(4d,5s) → Au(6s,6p) and Au(5d) → Au(6s,6p). Overall, there is a decrease in the 5d population of gold that should induce positive binding energy shifts in the Au 4f core levels and Au 5d band [28,54–56], as seen in Fig. 3. At the same time, the formation of Mo–Au bonds leads to a decrease in the net electron density on Mo [28], which should reduce the ability of this metal to donate electrons into the $2\pi^*$ orbitals of CO. A reduction of the so-called π-back donation would result in weaker Mo–CO bonds and make difficult the dissociation of CO [18,57,58]. In accordance with our results, experimental and theoretical studies for the dissociation of CH_4 on $Ni_{1-x}Au_x$(1 1 1) surfaces show a decrease in the chemical activity of nickel as a consequence of Ni–Au bonding [59].

The data in Fig. 2 indicate that Mo recovers its ability to dissociate CO at large metal coverages on the Au(1 1 1) substrate. As the Mo coverage increases, the Mo–Mo interactions become more important than the Mo–Au interactions, and the effects of bimetallic bonding are "diluted". In this respect, the "length scale" of the system is important, and special chemical properties are only observed for small Mo nanoparticles. These systems are still able to dissociate thiophene. On extended Mo surfaces, thiophene is a molecule much

more reactive than CO. On Mo(1 1 0) and Mo(1 0 0), thiophene decomposes at temperatures well below 200 K [26,33], whereas the dissociation of CO takes place at temperatures above 400 K [23,31].

The most important industrial application of MoS_2 catalyst involves HDS processes, where sulfur-containing molecules are removed from petroleum by reaction with hydrogen to form H_2S and hydrocarbons [5–8]. In HDS reactions, a key issue is the cleavage of C–S bonds by the catalyst [5–8]. Due to its large chemical stability, thiophene is a typical test molecule in desulfurization studies [5,13,25,26,33,60,61]. It is known that the sulfur basal plane of molybdenum sulfide, MoS_2(0 0 0 2) surface, interacts weakly with thiophene [60,61]. The adsorption energy of the molecule is only 9.5 kcal/mol, and desorption takes place at temperatures lower than 200 K [60]. Somewhat stronger bonding interactions have been observed for thiophene on MoS_x films [62] and MoS_x/Al_2O_3 catalysts [25], from where the molecule desorbs at temperatures between 200 and 300 K. But in all these systems, there is no dissociation of thiophene. To see dissociation of C_4H_4S on bulk molybdenum sulfide, the exposed surface must contain Mo atoms with a relatively low coordination number [61,63]. This type Mo atoms can be near S vacancies in a basal plane or located in edge planes of the MoS_2 crystal structure [5–8].

MoS_x nanoclusters supported on Au(1 1 1) dissociate the thiophene molecule (Figs. 8 and 9). INDO/S and ab initio HF calculations have been used to examine the electronic properties of a series of clusters of molybdenum sulfide (Mo_5S_{10}, Mo_6S_{12}, Mo_8S_{18}, Mo_9S_{18}, $Mo_{12}S_{24}$ and $Mo_{18}S_{36}$) [13]. In general, clusters of molybdenum sulfide can expose adsorption sites or exhibit electronic states that are not seen on surfaces of bulk MoS_2 [13]. For example, recent density-functional calculations comparing a Mo_9S_{18} cluster and bulk MoS_2 show "extra" occupied electronic states in the cluster which have a relatively low stability and are ideal for bonding interactions with sulfur-containing molecules [64]. Theoretical studies [13, 64] predict weak bonding between thiophene and the S-basal plane of Mo_nS_{2n} clusters. On the other hand, the molecule bonds strongly to unsaturated Mo atoms in Mo_nS_{2n-x} clusters that resemble atoms in edge planes of bulk MoS_2 [13,64]. On these adsorption sites there is a substantial weakening and elongation of the thiophene C–S bonds [13,64], making them good candidates to carry out the decomposition chemistry seen in Figs. 8 and 9.

5. Conclusions

$Mo(CO)_6$ can be useful as a precursor for the preparation of Mo and MoS_x nanoparticles on a Au(1 1 1) substrate. On this surface the carbonyl adsorbs intact at 100 K and desorbs at temperatures lower than 300 K. Under these conditions, the dissociation of the $Mo(CO)_6$ molecule is negligible and a desorption channel clearly dominates. An efficient dissociation channel was found after dosing $Mo(CO)_6$ at high temperatures (>400 K). The decomposition of $Mo(CO)_6$ yields the small coverages of pure Mo that are necessary for the formation of Mo nanoclusters on the Au(1 1 1) substrate. At large coverages of Mo (>0.15 ML), the dissociation of $Mo(CO)_6$ produces also C and O adatoms.

Mo nanoclusters bonded to Au(1 1 1) exhibit a surprising low reactivity towards CO. Mo/Au(1 1 1) surfaces with Mo coverages below 0.1 ML adsorb the CO molecule weakly (desorption temperature < 400 K) and do not induce C–O bond cleavage. These systems, however, are able to induce the dissociation of thiophene at temperatures below 300 K and react with sulfur probably to form MoS_x nanoparticles. The formed MoS_x species are more reactive towards thiophene than extended MoS_2(0 0 0 2) surfaces, MoS_x films or MoS_x/Al_2O_3 catalysts. This could be a consequence of special adsorption sites and/or distinctive electronic properties that favor bonding interactions with sulfur-containing molecules.

Acknowledgements

This research was carried out at Brookhaven National Laboratory under contract DE-AC02-

98CH10086 with the US Department of Energy (Division of Chemical Sciences). The National Synchrotron Light Source is supported by the Materials and Chemical Sciences Divisions of the US Department of Energy.

References

[1] O. Weisser, S. Landa, Sulfide Catalysts: Their Properties and Applications, Pergamon Press, Oxford, 1973.
[2] J.G. Speight, The Chemistry and Technology of Petroleum, second ed., McGraw-Hill, New York, 1991.
[3] J.G. Santiesteban, Ph.D. Thesis, Lehigh University, Bethelehem, PA, 1989.
[4] K.I. Tanaka, T. Okuhari, J. Catal. 78 (1982) 155.
[5] H. Tøpsoe, B.S. Clausen, F.E. Massoth, Hydrotreating Catalysis, Springer, New York, 1996.
[6] A.N. Startsev, Catal. Rev. Sci. Eng. 37 (1995) 353.
[7] R.R. Chianelli, M. Daage, M. Ledoux, Adv. Catal. 40 (1994) 177.
[8] B. Dellmon, Bull. Soc. Chim. Belg. 104 (1995) 173.
[9] C.H. Bartholomew, P.K. Agrawal, J.R. Katzer, Adv. Catal. 31 (1982) 135.
[10] A.C. Stern, R.W. Boubel, D.B. Turner, D.L. Fox, Fundamentals of Air Pollution, second ed., Academic Press, Orlando, FL, 1984.
[11] T.G. Kaufmann, A. Kaldor, G.F. Stuntz, M.C. Kerby, L.L. Ansell, Catal. Today 63 (2000) 77.
[12] S. Helveg, J.V. Lauritsen, E. Lægsgaard, I. Stensgaard, J.K. Nøskov, B.S. Clausen, H. Tøpsoe, F. Besenbacher, Phys. Rev. Lett. 84 (2000) 951.
[13] J.A. Rodriguez, J. Phys. Chem. B 101 (1997) 7524.
[14] K.G. Huang, D. Gibbs, D.M. Zehner, A.R. Sandy, S.G.J. Mochrie, Phys. Rev. Lett. 65 (1990) 3313.
[15] J.V. Barth, H. Brune, G. Ertl, R.J. Behm, Phys. Rev. B 42 (1990) 9307.
[16] Y. Hagsegawa, P. Avouris, Science 258 (1992) 1763.
[17] J. Hrbek, R.Q. Hwang, Curr. Opin. Solid State Mater. Sci. 5 (2001) 67.
[18] J.A. Rodriguez, Surf. Sci. Rep. 24 (1996) 232.
[19] D.D. Chambliss, R.J. Wilson, S. Chiang, Phys. Rev. Lett. 66 (1991) 1721.
[20] B. Vigtlander, G. Meyer, N.B. Amer, Surf. Sci. 255 (1991) L529.
[21] C.J. Baddeley, R.M. Ormerod, A.W. Stephenson, R.M. Lambert, J. Phys. Chem. 99 (1995) 5146.
[22] J. Wang, M.R. Voss, H. Busse, B.E. Koel, J. Phys. Chem. B 102 (1998) 4693 and references therein.
[23] G.A. Somorjai, Introduction to Surface Chemistry and Catalysis, Wiley, New York, 1994.
[24] G.A. Rizzi, R. Zanoni, S. Di Siro, L. Perriello, G. Granozzi, Surf. Sci. 462 (2000) 187.
[25] T.L. Tarbuck, K.R. McCrea, J.W. Logan, J.L. Heisler, M.E. Bussell, J. Phys. Chem. B 102 (1998) 7845.
[26] J.A. Rodriguez, J. Dvorak, T. Jirsak, Surf. Sci. 457 (2000) L413.
[27] I.J. Malik, J. Hrbek, J. Electron. Spectros. Rel. Phenom. 54/55 (1990) 479.
[28] J.A. Rodriguez, M. Kuhn, Surf. Sci. 330 (1995) L657.
[29] W. Heegeman, K.H. Meisner, E. Betchold, K. Hayek, Surf. Sci. 49 (1975) 161.
[30] J.A. Rodriguez, J. Hrbek, M. Kuhn, T. Jirsak, S. Chaturvedi, A. Maiti, J. Chem. Phys. 113 (2000) 11284.
[31] J.-W. He, W.-L. Shea, X. Jiang, D.W. Goodman, J. Vac. Sci. Technol. A 8 (1990) 2435.
[32] G. Liu, J.A. Rodriguez, J. Dvorak, J. Hrbek, T. Jirsak, J. Phys. Chem. B, submitted.
[33] F. Zaera, E.B. Kollin, J.L. Gland, Surf. Sci. 184 (1987) 75.
[34] J.A. Rodriguez, T. Jirsak, S. Chaturvedi, J. Chem. Phys. 110 (1999) 3138.
[35] S.Y. Li, J.A. Rodriguez, J. Hrbek, H.H. Huang, G.-Q. Xu, Surf. Sci. 366 (1996) 29.
[36] J.A. Rodriguez, S.Y. Li, J. Hrbek, H.H. Huang, G.-Q. Xu, Surf. Sci. 370 (1997) 85.
[37] W. Jaegermann, D. Schmeisser, Surf. Sci. 165 (1986) 143.
[38] E.L. Muetterties, Science 196 (1977) 839.
[39] B.C. Gates, H.H. Lamb, J. Mol. Catal. 52 (1989) 1.
[40] M.S. Nashner, A.I. Frenkel, D. Somerville, C.W. Hills, J.R. Shapley, R.G. Nuzzo, J. Am. Chem. Soc. 120 (1998) 8093 and references therein.
[41] D.C. Mancini, P. Skytt, J. Nordgren, P. Tagtstrom, Vacuum 46 (1995) 1165, and references therein.
[42] F.G. Celii, P.M. Whitmore, K.C. Janda, J. Phys. Chem. 92 (1988) 1604.
[43] K. Kishi, Y. Motoyoshi, S. Ikeda, Surf. Sci. 105 (1981) 313.
[44] J.L. Gland, R.W. McCabe, G.E. Mitchell, Surf. Sci. 127 (1983) L123.
[45] M. Xu, F. Zaera, J. Vac. Sci. Technol. A 14 (1996) 415.
[46] S.K. Clowes, A.E. Seddon, E.M. McCash, Surf. Sci. 464 (2000) L667.
[47] J. Vaari, J. Lahtinen, P. Hautojarvi, Surf. Sci. 346 (1996) 11.
[48] Z.C. Ying, W. Ho, J. Chem. Phys. 93 (1990) 9077.
[49] S.K. So, W. Ho, J. Chem. Phys. 95 (1991) 656.
[50] F. Zaera, J. Phys. Chem. 96 (1992) 4609.
[51] F.A. Flitsch, J.R. Swanson, C.M. Friend, Surf. Sci. 245 (1991) 85.
[52] T. Moeller, Inorganic Chemistry, Wiley, New York, 1982, p. 82–83.
[53] T.K. Sham, M.L. Perlman, R.E. Watson, Phys. Rev. B 19 (1979) 539.
[54] R.E. Watson, J.W. Davenport, M. Weinert, Phys. Rev. B 35 (1987) 508.
[55] T.K. Sham, Y.M. Yiu, M. Kuhn, K.H. Tan, Phys. Rev. B 41 (1990) 11881.
[56] M. Kuhn, T.K. Sham, Phys. Rev. B 49 (1994) 1647.
[57] J. Rodriguez, Surf. Sci. 303 (1994) 366.
[58] B. Hammer, Y. Morikawa, J. Nørskov, Phys. Rev. Lett.76 (1996) 2141.

[59] F. Besenbacher, I. Chorkendorff, B.S. Clausen, B. Hammer, A.M. Molenbroek, J.K. Nørskov, I. Stensgaard, Science 279 (1998) 1913.
[60] M. Salmeron, G.A. Somorjai, A. Wold, R. Chianelli, K.S. Liang, Chem. Phys. Lett. 90 (1982) 105.
[61] S.L. Peterson, K.H. Schulz, Langmuir 12 (1996) 941.
[62] J.A. Rodriguez, J. Dvorak, A.T. Capitano, A.M. Gabelnick, J.L. Gland, Surf. Sci. 429 (1991) L462.
[63] J.A. Rodriguez, J. Dvorak, T. Jirsak, S.Y. Li, J. Hrbek, A.T. Capitano, A.M. Gabenlnick, J.L. Gland, J. Phys. Chem. B 103 (1999) 5550.
[64] J.A. Rodriguez, to be published.